Colloids and Surfaces A 574 (2019) 12–20

Contents lists available at ScienceDirect

Colloids and Surfaces A

journal homepage: www.elsevier.com/locate/colsurfa

Controlling dispersion, stability and polymer content on PDEGMA-functionalized core-brush silica colloids

María Jazmín Penelas[a,b,1], Cintia Belén Contreras[a,c,1], Juan M. Giussi[c], Alejandro Wolosiuk[b], Omar Azzaroni[c], Galo J.A.A. Soler Illia[a,*]

[a] Instituto de Nanosistemas, Universidad Nacional de San Martín-CONICET, Av. 25 de Mayo 1021, San Martín, Buenos Aires, Argentina
[b] Gerencia Química, CAC-CNEA-CONICET, Av. Gral. Paz 1499, San Martín, Buenos Aires, Argentina
[c] Instituto de Investigaciones Fisicoquímicas Teóricas y Aplicadas, Universidad Nacional de La Plata-CONICET, Diagonal 113 y 64 S/N La Plata, Buenos Aires, Argentina

GRAPHICAL ABSTRACT

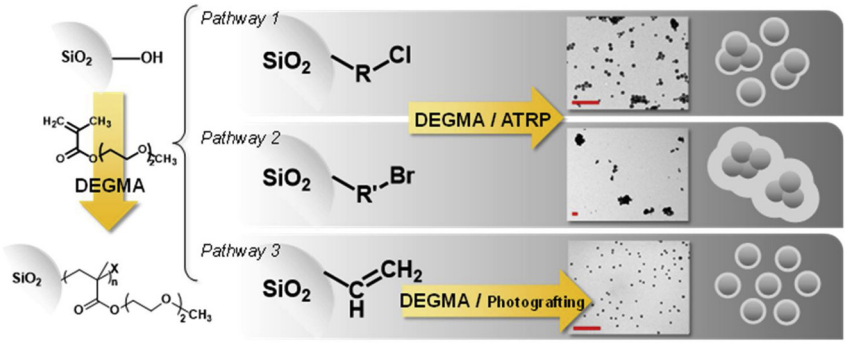

ARTICLE INFO

Keywords:
Hybrid materials
Core-brush nanoparticles
Responsive silica colloids
Functional polymer brushes
PEG-functionalized colloids

ABSTRACT

Core-brush hybrid nanoparticles containing PEG surface functions are highly interesting as biologically inert and smart stimuli-responsive materials for future applications in biosensors, drug delivery, tissue engineering and optical systems. In this context, surface modification methodologies are critical to exert a thorough control of morphological and functional aspects such as grafting density, polymer conformation or colloidal dispersability. In this work, we present core-brush hybrid nanoparticles synthesis from SiO_2 particles and an oligo(ethyleneglycol)-based polymer. Di(ethylene glycol) methyl ether methacrylate (DEGMA) was successfully grafted using the *grafting-from* approach. In particular, we compared DEGMA grafting on SiO_2 particles using three pathways, where route 1 and 2 corresponds to a surface-initiated atom radical polymerization (SI-ATRP), while pathway 3 consists in a photo-grafting polymerization. The polymer density grafted on the SiO_2 surface, as well as the dispersion and stability of the core-brush particles colloid system were investigated. We demonstrate that although all the methodologies were successful in immobilizing the PDEGMA on the surface, selection of the synthetic route is key to control crucial characteristics of core-brush NPs such as grafted polymer density, dispersion and colloidal stability. The accurate control of these critical features through the synthesis pathway is of great importance for the performance of these novel materials.

* Corresponding author at: Instituto de Nanosistemas, Universidad Nacional de San Martín, Av. 25 de Mayo 1021, San Martín, Buenos Aires, Argentina.
E-mail address: gsoler-illia@unsam.edu.ar (G.J.A.A. Soler Illia).
[1] M.J.P. and C.B.C. contributed equally to this work.

https://doi.org/10.1016/j.colsurfa.2019.04.035
Received 8 February 2019; Received in revised form 30 March 2019; Accepted 15 April 2019
Available online 20 April 2019
0927-7757/

1. Introduction

Organic-inorganic hybrid nanoparticles are essential functional components for advanced applications in fields ranging from nanomedicine to food packaging and catalysis [1]. Organic–inorganic hybrid materials can be tailor-made with an infinite number of architectures and in diverse physical forms depending on the requirements of their final application, adjusting conveniently the starting materials and the strategies of synthesis and functionalization [1–7]. Core-brush particles, consisting in covalently graft polymer chains onto the inorganic core, have attracted increasing interest, since they can be obtained with high particle size control, dispersibility and functionality [8]. In these hybrid nanomaterials, the properties of the inorganic core and the organic polymer shell are combined, resulting in a new class of materials that exhibit improved performance for the design and control of the properties of polymers and surfaces compared to their microparticle counterparts [9–14]. In this context, several research works have shown that the dispersibility, the degree of particle aggregation and the nanoparticle surface chemistry are key parameters for the control of the stability, structure, physical and mechanical properties of nanocomposites, suspensions, foams and mixtures of polymers, maintaining the cohesion between the particles and the host matrix under shearing or thermal constraint [8,15,16].

Among the various inorganic oxides, silica particles have received much attention due to their, high surface area, cost-effective production, and the simple surface modification, biocompatibility and cost-effective production [14,17–22]. Functionalization of the silica surface can be carried out in a straightforward fashion by controlling the reactivity of silanol species (-SiOH) with organosilicon alkoxides in different media. The grafted organic moieties play a critical role in the specific properties of the resulting hybrid materials, such as chemical binding ability, surface charge, hydrophobicity and colloidal stability, and can be further derivatized with other useful functionalities [14]. Functional polymer brushes have been successfully grafted to the surface from a rich library of monomer species by following either conventional free or controlled radical polymerization, with the aim to modified the nanoparticle surface [23]. In this sense, up to now, many efficient techniques have been reported for the successful implementation of the "*grafting from*" approach [23].

Non-controlled radical polymerizations generally present some advantages, for example involve simple equipment, low cost of processing, fast reaction rate and therefore, they are the most viable since an industrial scalability point of view [18,24]. However, controlled radical polymerizations allow a better control of the molecular weight and the polydispersion of grafted polymer chains, producing well-defined architectures [25,26]. The application of these two types of radical polymerization through specific methodologies, allowed creating a wide diversity of core-brush structures from SiO_2 NPs and monomers of different nature. For example, Van Nguyen et al., analyzed the kinetics of the process of the free-radical graft polymerization of 1-Vinyl-2-pyrrolidone onto vinyltrimethoxysilane (VTMS) modified silica via a model that incorporates the hybrid cage–complex initiation mechanism [27]. More recently, Khoonsap et al., studied the grafting of poly(2-hydroxyethyl methacrylate) on silica nanoparticles via the sequential UV-induced graft polymerization [28]. On the other hand, using a controlled polymerization, Du and co-workers prepared thermosensitive SiO_2 nanoparticles with brushes of poly(ethylene glycol) methyl ether methacrylate (POEGMA) on its surface via atom transfer radical polymerization (ATRP) [29].

Poly(ethylene glycol) (PEG) and its derivatives exhibit many unique physical and biochemical properties, such as uncharged, non-toxicity, non-immunogenesis, non-antigenicity, excellent biocompatibility, protein-resistant and miscibility with many solvents and have been widely applied in biomedical applications [30–33]. In addition, the thermosensitive nature of PEG-based surface chains was recently proposed as an attractive alternative to traditional poly(n-isopropylacrylamide), PNIPAm. For example, random copolymers of 2-(2-methoxyethoxy) ethyl methacrylate (MEO_2MA, n = 2) and oligo(ethylene glycol) methacrylate (OEGMA, n~9) exhibit lower critical solution temperature (LCST) tunable values between 26 °C and 90 °C. The LCST can be precisely adjusted by varying the length of the oligo(ethylene oxide) side chain [34]. Conventional methods for immobilizing PEG brushes on substrates include adsorption of PEG block copolymers at multiple sites on the surface, direct attachment of self-assembled PEG monolayer to surfaces, functionalization with organosilanes containing PEG as organic moiety and graft polymerization of PEG monomers to a polymer backbone. For example, Shin and collaborators reported the successful modification surface silica nanoparticles with poly(ethylene glycol) methacrylate (PEGMA) or poly(propylene glycol) methacrylate (PPGMA) using *grafting from* approach on the particle surface via UV-photopolymerization [35].

It is important to emphasize that the controlled surface modification of silica nanoparticles is not trivial and the reaction conditions and reagents must be carefully chosen depending on the final purpose. The effectiveness of each strategy to build a surface that exhibits the properties required depends not only on the intrinsic properties of the grafted functional chain, but also on molecular structure and surface coverage. Although a considerable attention has been focused on the successful particle surface modification by different *graft* polymerization, the conditions for achieving dispersion control, colloidal stability and polymer content in hybrid silica nanoparticles are still not sufficiently established. This constitutes a limitation for the actual design of precisely controlled core-brush nanopartciles. In this article we report the development and synthesis of core-brush nanoparticles via *grafting-from* approach. For this, poly di(ethyleneglycol) methyl ether methacrylate (PDEGMA) was successfully grafted on SiO_2 nanoparticles by two frequently used *graft* polymerization techniques, surface-initiated atom transfer radical (SI-ATRP) and UV photo-initiated polymerization. The obtained results demonstrated that although all the methodologies addressed were successful in immobilizing the PDEGMA on the surface, key characteristics for core-brush NPs performance in the desired application, such as grafted polymer density, dispersion and the colloidal system stability showed significant differences.

2. Materials and methods

2.1. Materials

Tetraethylorthosilicate (98%, TEOS), chloropropyltriethoxysilane (95%, CPTES), vinyltriethoxysilane (97%, VTES), *N,N*-diisopropylethylamine (99%, DIPEA), (3-aminopropyl) triethoxysilane (99%, APTES), 2-bromopropionyl bromide 97%, di(ethylene glycol) methyl ether methacrylate (95%, DEGMA), 2,2′-bipyridine (99%, biPy), copper (I) bromide (99.9%, CuBr), 2,2-dimethoxy-2-phenylacetophenone (99%, DMPA) were purchased from Sigma-Aldrich. Concentrated aqueous ammonia and absolute ethanol were obtained from Biopack and toluene and methanol were purchased from Merck. All chemicals were used as received. Water used was deionized (18 MΩ cm) and filtered. *N*-(triethoxysilyl)propyl-2-bromopropanamide (BPATES) was prepared following the methodology previously reported by Tugulu et al. [36]

2.2. Hybrid nanomaterials preparation

2.2.1. Synthesis of SiO_2 nanoparticles

Silica nanoparticles were prepared according to the Stöber method [37]. A portion of TEOS was added under vigorous stirring to a mixture containing absolute ethanol, deionized water and concentrated aqueous ammonia. The final molar concentrations were TEOS 0.17 M, $NH_3.H_2O$ 0.75 M and H_2O 2 M. The mixture was stirred overnight at room temperature. Afterwards, in case of CPTES and BPATES functionalization, the suspension was exposed to the following steps: it was distilled under vacuum by a rotary evaporator (thermostatic bath temperature 52 °C,

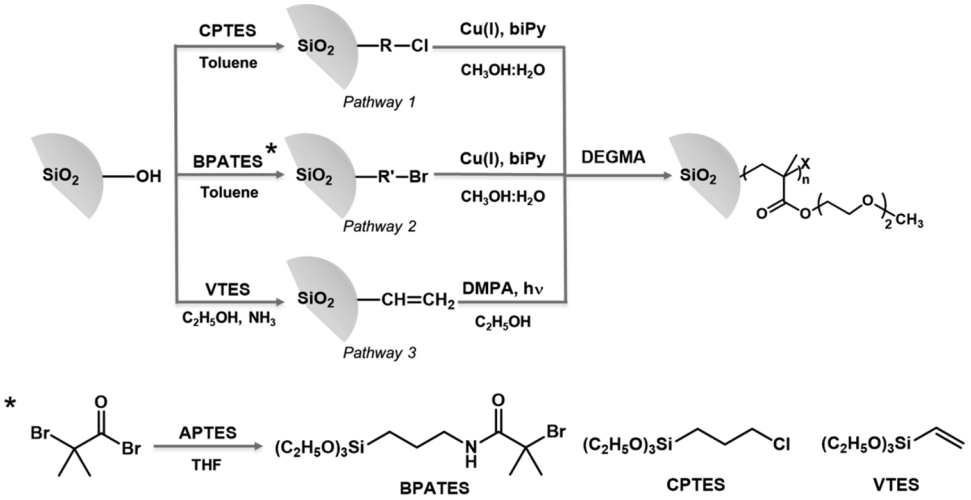

Scheme 1. Surface modification on SiO_2 NPs by PDEGMA grafting. *BPATES (*N*-(triethoxysilyl)propyl-2-bromopropanamide) synthesis.

pressure closer to 19 kPa) in order to remove ammonia and water, until suspension pH was 6–7 and extra ethanol was added to prevent the suspension from drying out. The NPs were washed with 0.1 M HCl in order to hydrolyze the surface -$SiOC_2H_5$ remaining groups from the synthesis, followed by several washes with water until neutral pH; each wash using centrifugation cycles at 8000 rpm for 15 min and re-suspension by sonication. The washed NPs were dried in vacuum at room temperature for 72 h. While, in case of functionalization with VTES, the suspension resulting from the Stöber synthesis was used without further treatment for the next steps.

Typically, the amount of SiO_2 and modified SiO_2 NPs employed in the following syntheses was around 100 mg (1% m/v suspension). Surface modification of these SiO_2 NPs was performed in three routes as shown in Scheme 1. For each route, the synthesis conditions studied were carried out at least twice for reproducibility evaluation.

2.2.2. Pathway 1– surface-initiated ATRP of DEGMA on SiO_2-Cl NPs

2.2.2.1. Immobilization of ATRP initiator (CPTES) on SiO_2 NPs surface, SiO_2-Cl NPs preparation. The dry SiO_2 NPs were redispersed in toluene after 30 min sonication (1% m/v suspension). Subsequently, DIPEA was added reaching a 0.14 M, and the suspension was stirred at 60 °C. CPTES was added and allowed to react under stirring overnight. The amount of CPTES used in the synthesis corresponds to 50 times the one required to cover the SiO_2 NPs surface with a monolayer of organic silane agent, assuming a grafting density of 2 molecules/nm^2 and a density of the SiO_2 NP of 1.58 g/cm^3 [38]. The exposed surface area was estimated from the hydrodynamic diameter obtained by DLS. Afterwards, the necessary amount of ethanol was added to the suspension to completely remove toluene by azeotropic distillation with a rotary evaporator. The SiO_2-Cl NPs obtained by silanization with CPTES were washed three times by dispersion-centrifugation (5000 rpm, 15 min) with ethanol and dried under vacuum during 72 h at room temperature.

2.2.2.2. Synthesis of (SiO_2-Cl)-g-PDEGMA NPs. The dry SiO_2-Cl NPs were resuspended in methanol by a sonication process during 30 min in a Schlenk tube diluted in half with deionized water (0.25% m/v suspension). Then, the ligand 2,2′-biPy and the monomer DEGMA were added. Nitrogen was bubbled during 30 min in order to degas the system. Finally, CuBr was added under N_2 and it was bubbled during 15 min. The reactants were added in the following molar ratio with respect to the CPTES used in the functionalization: CPTES: 2,2′-biPy: CuBr: DEGMA 1: 1: 1: 50. The reaction was carried out at 25 °C overnight (polymerization was stopped by opening the flask to permit air to enter). Finally, the hybrid nanoparticles (SiO_2-Cl)-*g*-PDEGMA type core-brush were obtained with brushes of poly(DEGMA), PDEGMA. The NPs were washed and recovered by six dispersion-centrifugation cycles (4500 rpm, 15 min) in ethanol-water in order to eliminate the non-attached monomer. Finally, the NPs were washed and recovered with HCl 0.1 M (once) and water (two portions) in order to remove the complex CuBr-biPy (See supporting information Figure S1). The (SiO_2-Cl)-*g*-PDEGMA NPs were dispersed in ethanol to obtain a stock suspension 5% w/v.

2.2.3. Pathway 2 – surface-initiated ATRP of DEGMA on SiO_2-Br

2.2.3.1. Synthesis and immobilization of N-(triethoxysilyl)propyl-2-bromopropanamide (BPATES, ATRP initiator) on SiO_2 NPs, SiO_2-Br NPs preparation. Synthesis: *N*-(triethoxysilyl)propyl-2-bromopropanamide (BPATES) was prepared following the methodology previously reported by Tugulu et al. [36] Briefly, 2-bromoisobutyryl bromide (3 mL, 24 mmol) was added slowly and under ice cooling to a solution of 3-aminopropyltrimethoxysilane (3.5 mL, 20 mmol) and triethylamine (3.35 mL, 24 mmol) in 30 mL of anhydrous tetrahydrofuran (THF). The solution was allowed to warm to room temperature and stirring was continued for 3 h. The reaction was carried out under nitrogen atmosphere and then the product was purified and characterized by ^{1}H-NMR and ^{13}C-NMR.

^{1}H-NMR (400 MHz, $CDCl_3$) δ 6.87 (s, 1 H), 3.53 (s, 9 H), 3.22 (m, 2 H), 1.91 (s, 6 H), 1.62 (m, 2 H), 0.62 (t, J = 8.12 Hz, 2 H). ^{13}C-NMR (100 MHz, $CDCl_3$) δ 6.3, 22.5, 32.4, 42.6, 50.5, 62.5, 77.4, 171.8.

Immobilization: The dry SiO_2 NPs were redispersed in the majority portion of the total dry toluene volume to be used and then BPATES was dissolved in the remaining part of the solvent, and it was added. The amount of BPATES used in the functionalization followed the criteria previously applied with CPTES, and the final concentration of the suspension was 1,7% m/v. The mixture was allowed to react under stirring at 100 °C for 2 h, and then at room temperature overnight. The SiO_2-Br NPs were washed three times by dispersion-centrifugation (5000 rpm, 15 min) with ethanol and they were dried under vacuum during 72 h at room temperature.

2.2.3.2. Synthesis of (SiO_2-Br)-g-PDEGMA NPs. The procedure used was similar to that followed to obtain the (SiO_2-Cl)-*g*-PDEGMA NPs: briefly, 2,2′-biPy and DEGMA were added to a suspension 0.25% m/V of the SiO_2-Br NPs in MeOH : H_2O 1 : 1 while CuBr was added in a later step. N_2 bubbling was constatnt during along this procedure. The molar proportions are those previously indicated for Pathway 1. The reaction was carried out at 25 °C during 4 h. The hybrid NPs (SiO_2-Br)-*g*-PDEGMA obtained with brushes of PDEGMA were washed and recovered by the procedure outlined above, and they were dispersed

in ethanol to obtain a stock suspension 5% w/v.

2.2.4. Pathway 3 - photografting of DEGMA on SiO_2-V NPs

2.2.4.1. VTES immobilization on SiO_2 NPs, SiO_2-V NPs preparation. The SiO_2-V NPs were synthesized from the bare SiO_2 NPs suspension previously obtained, notice that this silanization process was carried out one-pot. The volume of VTES, calculated as in previous silanizations, was added to the SiO_2 synthesis suspension under stirring, and allowed to react overnight at room temperature. The SiO_2-V suspension was then distilled under vacuum using a rotary evaporator to remove ammonia and water, until suspension pH was 6–7. Excess of VTES was removed after two cycles of dispersion-centrifugation (5000 rpm, 15 min) with fresh ethanol. The SiO_2-V NPs were dispersed in ethanol to obtain a stock suspension 10% w/v.

2.2.4.2. Synthesis of (SiO_2-V)-g-PDEGMA NPs. In a glass vial, monomer, DEGMA, and photo-initiator, DMPA, were dissolved in absolute ethanol and then the necessary amount of the stock suspension of SiO_2-V NPs was added. The molar ratio used with respect to the VTES used in the functionalization was VTES: DMPA: DEGMA 1: 0.01: 50 and the final concentration in NPs of the reaction suspension was 1.1% w/v. In order to degas the system, nitrogen was bubbled during 30 min. Afterwards, the reaction suspension was irradiated under stirring using a 15 W, 18″-long black-light lamp (λ_{max} = 352 nm) overnight at room temperature. The polymerization was stopped by turning off the lamp and by opening the vial to permit air to enter. Finally, the obtained NPs were washed and recovered by dispersion-centrifugation cycles (4500 rpm, 15 min) in acetone (four portion) and ethanol (two portion) for eliminate the non-attached components. The (SiO_2-V)-*g*-PDEGMA NPs were dispersed in ethanol to obtain a stock suspension 5% w/v.

2.3. Equipment and characterization techniques

2.3.1. FTIR measurements

Infrared Fourier transform spectroscopy measurements were performed with a Nicolet Magna 560 instrument, equipped with liquid N_2 cooled MCT-A detector in DRIFTS mode. Samples were prepared mixing SiO_2 or modified SiO_2 NPs, previously dried under vacuum during 72 h, with KBr until reach a final composition of 3% w/w.

2.3.2. Thermogravimetric analysis

TGA data were obtained from TA Instruments – TGA Q500 equipment, under nitrogen flux (50 mL.min^{-1}), in sealed alumina pans heated up to 800 °C (10 °C.min^{-1}).

The estimated number of surface grafted groups per area unit (N_{exp}) and percentage of grafting (*%G*) of modified SiO_2 NPs by polymer was calculated using TGA data according to Eqs. 1 and 2 respectively. Where, m_{org} is the final mass difference, m_{inorg} is the remaining inorganic mass, S_{NP}, V_{NP} and ρ correspond to the surface, volume and density of the SiO_2 NPs from geometric estimations, N_A is the Avogadro's number, M_{org} is the molecular weight of the incorporated organic group and m_0 is initial mass. For the nanoparticle density, ρ, we assumed a value of 1.58 g/cm^3 from literature. [12,28,38]

$$N_{exp} = \frac{\left(\frac{m_{org}}{m_{inorg}}\right)\rho V_{NP} N_A}{M_{org} S_{NP}} \quad (1)$$

$$\%G = 100\frac{m_{org}}{m_o} \quad (2)$$

2.3.3. Dynamic light scattering (DLS)

DLS measurement was performed in a BI-200SM Goniometer Ver. 2.0 (Brookhaven Instrument Corp.) scanning the range of 30-150° every 10° (λ = 637 nm). Samples were prepared by diluting a 50 μL aliquot of the NPs suspension in approximately 12 mL of ethanol, containing in a DLS glass vial. Hydrodynamic diameter (D_h) of the NPs was calculated using the Stokes-Einstein equation from the cumulant analysis from Brookhaven Instruments built-in software package. Polydispersity Index (PDI) was calculated from the cumulants analysis, and is dimensionless value of the broadness of the particle size distribution.

2.3.4. Microscopy images

Transmission electron microscopy (TEM) images were recorded using a Philips CM 200 electronic microscope operating at 180 kV equipped with an energy dispersive spectrometer (EDS). Samples were prepared by dropcasting, where the dried NPs were dispersed in ethanol. Then, drops of this dispersion were placed onto standard carbon-coated colodion film copper grids (200-mesh), which was followed by solvent evaporation. For each sample, a minimum of four different regions were studied. The estimated size of the NPs was calculated using the Image *J* public domain processing program.

2.3.5. Thermo-responsiveness study

The thermo-response behavior was evaluated using a (SiO_2-Br)-*g*-PDEGMA NPs aqueous colloid suspension (5% w/v), which was exposed to the temperature increasing from room temperature to 60 °C under constant stirring.

3. Results and discussion

The size-controlled SiO_2 NPs were obtained by the well-known Stöber method, from the sol-gel process of hydrolysis and subsequent condensation of a Si alkoxide precursor (TEOS, in this case) in aqueous ethanol, using ammonia as a catalyst [37]. The molar concentrations of TEOS, NH_3 and H_2O used in synthesis lead to obtaining NPs of approximately 100 nm as part of a monodisperse colloidal system.

Surface modification of these SiO_2 NPs was performed in three routes as shown in Scheme 1 (Materials and Methods Section 2.2); each one was divided in two steps. In the first step of the synthesis, the surface of SiO_2 NPs was functionalized by a reaction with an organic silane agent, which was subsequently used in a second step, as an initiator for grafting polymerization. After this, type core-brush NPs of SiO_2 were obtained with brushes of poly(DEGMA), PDEGMA. We decided to evaluate PDEGMA grafting on SiO_2 surface via two frequently *graft* polymerization techniques, surface-initiated atom transfer radical SI-ATRP and photopolymerization. Therefore, the difference between the three routes was the kind of polymerization and initiator. In pathways 1 and 2 SI-ATRP, was performed; while in pathway 3 a photopolymerization was carried out. Chloropropyltriethoxysilane, CPTES, was used as SI-ATRP initiator in pathway 1, while *N*-(triethoxysilyl)propyl-2-bromopropanamide BPATES was used in route 2. In case of pathway 3, vinyltriethoxysilane, VTES, was used as initiator. Notice that, in order to make a comparative study; in the three synthetic routes, the ratio of organic silane agent as initiator is the same, which corresponds to 50 monolayers, as well as the molar ratio initiator: monomer 1:50 for PDEGMA grafting. However, for each route, other conditions were evaluated, such as initiator ratio or reaction time, in order to understand the effect of the synthesis variables in different aspects of the materials.

Fig. 1 shows DRIFTS-FTIR spectra of unmodified and silanized SiO_2 NPs and the core-brush hybrid material produced. All the samples shows the broad absorption band at around 3800 − 3200 cm^{-1} and at 1640 cm^{-1}, originated by the stretching and bending vibrations of the O—H groups, respectively; as well as the strong absorption bands in 1200 − 800 cm^{-1} region due to the O-Si-O vibrations. After silanization, weak bands in the interval 1350-1550 cm^{-1} were observed due to stretching and deformation vibrations by the C—H bond of alkyl residues. In the case of BPATES silanization, an extra band in 1537 cm^{-1} appeared, due to N—H bending vibration of the amide group generated by the derivatization of the amino group of APTES. Notice that the

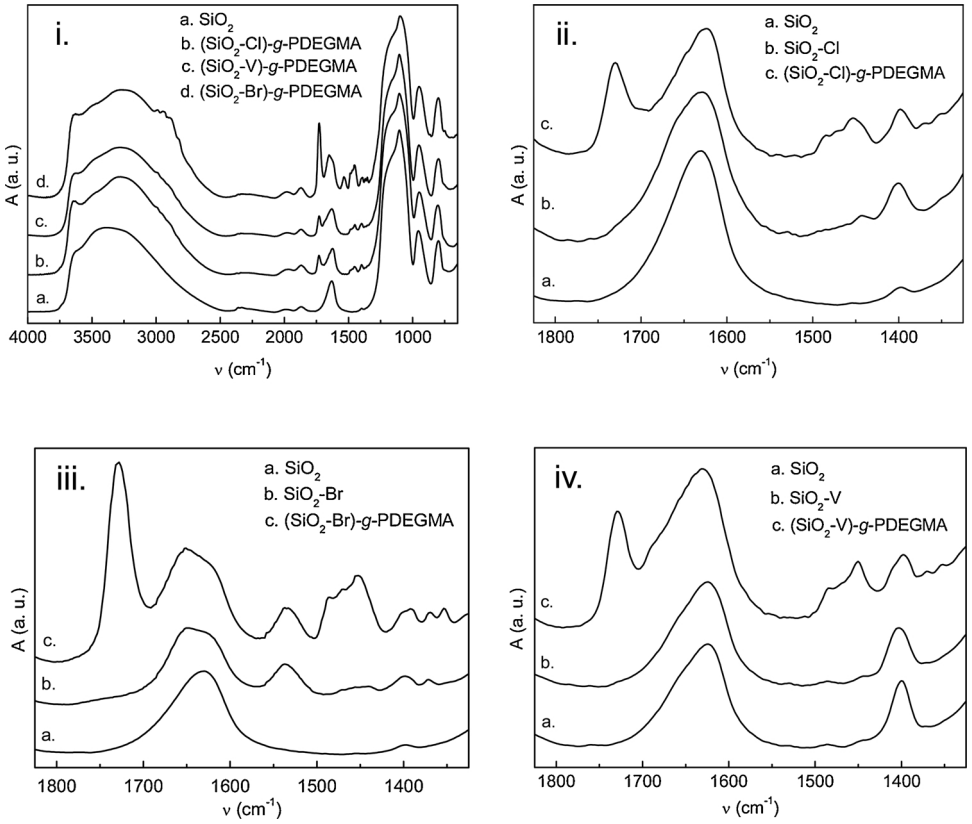

Fig. 1. DRIFTS-FTIR spectra of the PDEGMA core-brush NPs (i) and NPs spectra zoom in the different stages of each synthesis pathway (ii-iv).

signals from the C—H bond could be identified in the SiO_2 spectrum corresponding to pathway 3, which was attributed to remaining ethoxy groups present in the silica NPs due to the incomplete hydrolysis of the TEOS during the Stöber synthesis [39]. These absorption bands were not observed in spectrum corresponding to pathway 1 and 2, which was attributed to the removal of said groups by hydrolysis after washing with HCl solution.

Upon graft polymerization, other intense bands appeared in the DRIFTS spectra confirming the PDEGMA successfully grafting on functionalized SiO_2 particles. The main PDEGMA band observed corresponds to the stretching of -C = O at 1730 cm^{-1}, accompanied by the anti-symmetric and symmetric stretching modes of $-CH_2$, distinguishable at approximately 2929 and 2858 cm^{-1}, and an increase in the corresponding signals C—H vibrations around 1500 − 1430 cm^{-1}. Moreover, Fig. 1i shows a different relative intense 1730 cm^{-1} band depending on the core-brush material: (SiO_2-Cl)-*g*-PDEGMA and (SiO_2-V)-*g*-PDEGMA NPs presented similar intensity, while (SiO_2-Br)-*g*-PDEGMA showed the higher intensity. This result could be attributed to the highest polymer content in (SiO_2-Br)-*g*-PDEGMA NPs, due to the SI-ATRP was carried out using BPATES initiator on the SiO_2 surface. It is well know that BPATES leads to the formation of a dense polymer layer (brush) due to its good reactivity [40].

The thermal properties of bare, silanized and PDEGMA core-brush SiO_2 NPs were evaluated using TGA. Fig. 2 shows TGA data of (SiO_2-Br)-*g*-PDEGMA as a representative core-brush SiO_2 NPs with PDEGMA brushes system (for (SiO_2-Cl)-*g*-PDEGMA and (SiO_2-V)-*g*-PDEGMA TGA data see Supporting Information Figure S2). The weight loss observed for bare SiO_2 was around 10–15% when heated from room temperature to 800 °C, which was mainly caused by the elimination of strongly absorbed water up to approximately 200 °C, and then by various dehydroxylation processes [41]. After SiO_2 silanization with CPTES, BPATES and VTES, weight loss presented the same profile than bare SiO_2 NPs and significant differences were not observed. For the core-brush SiO_2 NPs with PDEGMA brushes, two distinct weight losses were

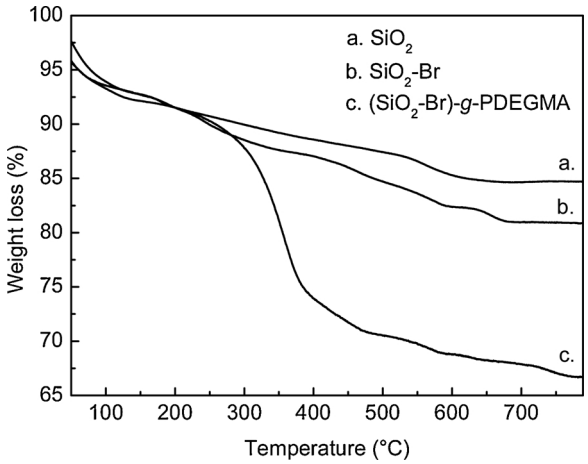

Fig. 2. TGA data of unmodified SiO_2 NPs, functionalized SiO_2, SiO_2-Br and SiO_2 NPs grafted with PDEGMA, (SiO_2-Br)-*g*-PDEGMA.

observed. The first weight loss was observed after heating to 200 °C, which was due to water being strongly absorbed [41]. The second weight loss took place between 200 and 600 °C, from a process corresponding to the progressive thermal decomposition of the remaining organic content. This occurred in several closely related but undistinguished stages, thereby making the assignation of the fragments impossible (monomers, dimers, etc,). From 600 °C, all thermograms remained mainly constant. The organic content of each system, as well as the organic loading achieved at each synthetic step, was calculated by taking into consideration the weight loss occurring from 200 °C.

The weight loss was 9.9, 24.7 and 9.8% for (SiO_2-Cl)-*g*-PDEGMA, (SiO_2-Br)-*g*-PDEGMA and (SiO_2-V)-*g*-PDEGMA, respectively. In addition, Table 1 shows the, estimated number of surface graphed groups per area unit, N_{exp}, and grafting percentage, %G calculated from

Table 1
Estimated number of surface-grafted groups per area unit, N_{exp}, and grafting percentage, %G calculated from thermogravimetric experiments.

	Nexp (nm^{-2})	%G
SiO_2-Cl	2.2	–
SiO_2-Br	6.4	–
SiO_2-V	15.6	–
(SiO_2-Cl)-*g*-PDEGMA	5.1	3.5
(SiO_2-Br)-*g*-PDEGMA	35.4	17.9
(SiO_2-V)-*g*-PDEGMA	4.3	3.4

thermogravimetric experiments. The N_{exp} value for silanized NPs in toluene did not show significant differences, while for one-pot silanized NPs the number was a bit higher. This result was consistent with the polycondensed organosilane networks bonding on the surface, a typical result in aqueous reaction media [42]. The (SiO_2-Br)-*g*-PDEGMA NPs presented the highest N_{exp} and %G, 35.4 nm^{-2} and 17.9%, respectively, while these parameters were similar for the SiO_2 NPs modified with PDEGMA brushes obtained by routes 1 and 3. Notice that this TGA results showed a good correlation with the intensity of the signals of the DRIFTS spectra data, where BPATES led to the formation of the dense polymer layer (brush) on the surface of SiO_2.

DLS provides valuable information of the level of aggregation and interaction between suspended particles in solution. Table 2 shows the hydrodynamic diameter (D_h) and the polydispersity index (PDI) values in absolute ethanol, obtained from NPs in each stage of synthesis for the three routes studied. Results show that for the different pathways, the D_h changed throughout all the synthesis steps. For pathway 1, the bare SiO_2 NPs presented a D_h of 154 ± 3 nm and a good PDI, indicating monodispersed NPs. When the SI-ATRP initiator, CPTES, was immobilized on SiO_2 surface, the D_h and PDI increased to 202 ± 3 and 0.144, respectively. This increase in average size, accompanied by a high PDI value, indicates the presence of particle clusters into the colloidal suspension, caused by the undesirable aggregation produced during the synthesis process. The values for the (SiO_2-Cl)-*g*-PDEGMA NPs D_h of 226 ± 25 nm and PDI 0.110, indicates that polydispersed aggregates continued into the colloid suspension. In the case of route 2, a similar and increased behavior was observed for SiO_2-Br and (SiO_2-Br)-*g*-PDEGMA NPs, for whose suspensions the level of aggregation was such that it was not possible to determine a particle size with this technique. Clearly, all stages of SI-ATRP grafting explored here led to irreversible formation of aggregates, especially during the silanization process. For example, notice that the CPTES and BPATES are not stable in aqueous ammonia medium, so the SiO_2 functionalization could not be performed in a one-pot procedure. Therefore, a set of separation, purification and resuspension operations in a new medium is necessary, which leads to the loss of colloidal stability. When the SiO_2 particles are dried under vacuum and resuspended in a non-polar solvent such as toluene, silanol groups are less ionized, and consequently the surface charge decreases, which causes destabilization of the colloidal system. In addition, functionalization with BPATES leads to colloidal aggregation, which can be attributed to an increase in the isoelectric point of the SiO_2 surface due to silanol replacement, as observed after APTES functionalization [43,44]. It is therefore highly probable that the poor resuspension of the NPs compromises the availability of the entire surface for functionalization, preventing the synthesis of individual NPs homogeneously modified on their surface with the polymer layer.

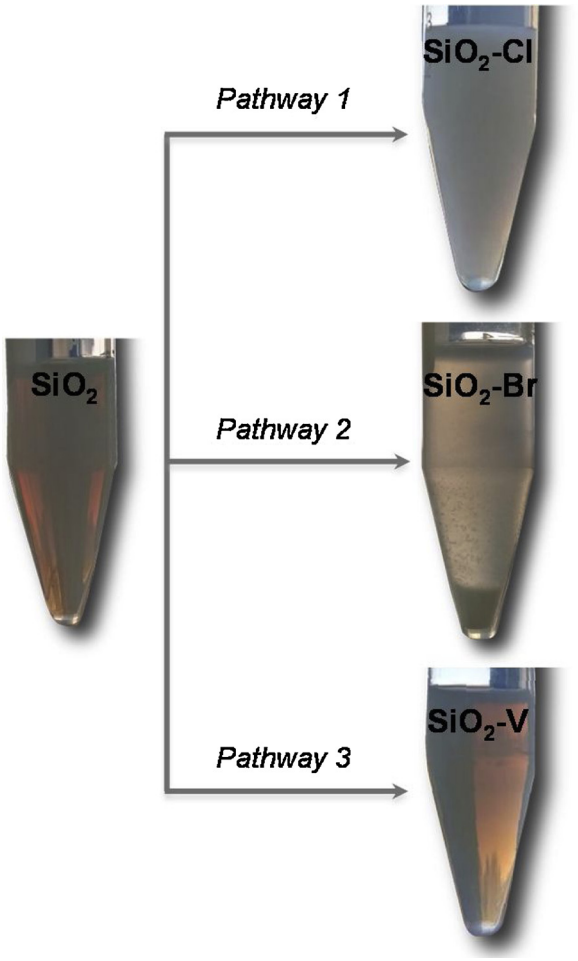

Fig. 3. Suspensions 5% w/v of unmodified SiO_2 NPs and functionalized SiO_2 NPs, SiO_2-Cl, SiO_2-Br, SiO_2-V. For each sample, hold up to the light (right).

On the other hand, Pathway 3 showed a markedly different behavior on the DLS experiments. The original D_h and PDI were conserved when SiO_2 NPs were functionalized by VTES. For (SiO_2-V)-*g*-PDEGMA NPs the D_h and PDI were 166 ± 3 nm and 0.073, respectively indicating good monodispersity of colloids suspension. The increased in D_h of 32 nm could be directly attributed to the brushes polymer presence on the SiO_2 NPs surfaces. This good behavior could be explained taking into account that the approach used for the synthesis (SiO_2-V)-*g*-PDEGMA NPs proceeds entirely in ethanol solution, solvent whereby both bare and modified SiO_2-V have great affinity, involves few separation steps and those that do not cause destabilization of the colloidal system [45].

The DLS results can be easily correlated with visual observations. Fig. 3 presents photographs of ethanol colloidal suspensions (5% w/v) of the unmodified SiO_2 and functionalized SiO_2 NPs with the three silane organic agents, CPTES, BPATES and VTES. In case of SiO_2 and SiO_2-V colloid suspensions exposed to the light showed similar scaterring properties. While, in the case of SiO_2-Cl and SiO_2-Br suspensions

Table 2
Hydrodynamic diameter and standard deviation, D_h ± SD (nm) and polidispersity index (PDI, in brackets), obtained by DLS of bare SiO_2, functionalized SiO_2, and grafted SiO_2 NPs. Agg. indicates aggregates.

Pathway 1	SiO_2	154 ± 3 (0.050)	SiO_2-Cl	202 ± 3 (0.144)	(SiO_2-Cl)-g-PDEGMA	226 ± 25 (0.110)
Pathway 2	**SiO_2**	165 ± 6 (0.070)	**SiO_2-Br**	Agg.	**(SiO_2-Br)-g-PDEGMA**	Agg.
Pathway 3	**SiO_2**	134 ± 4 (0.077)	**SiO_2-V**	134 ± 3 (0.079)	**(SiO_2-V)-g-PDEGMA**	166 ± 3 (0.073)

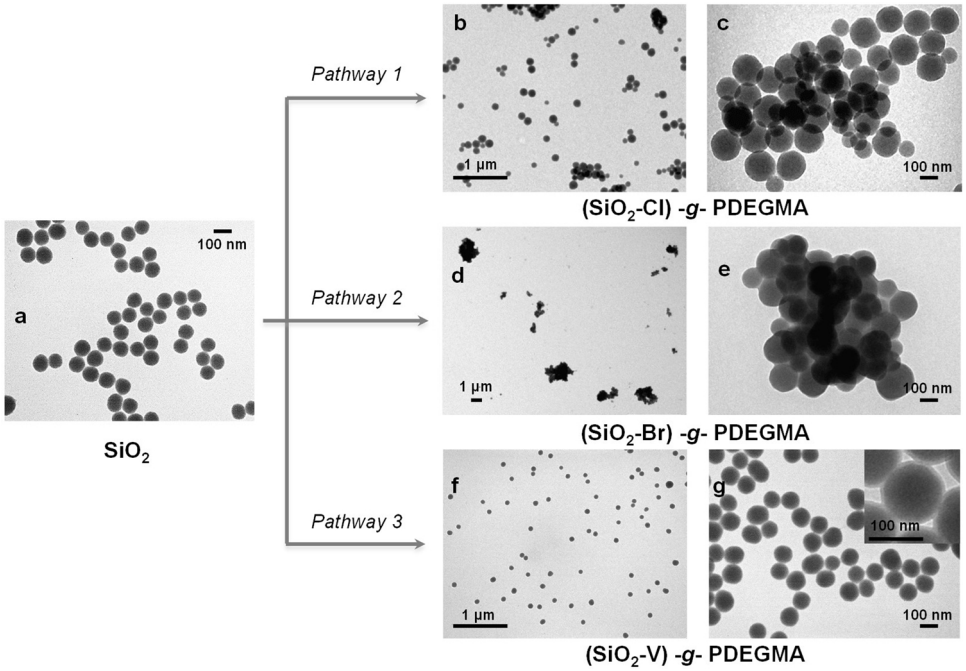

Fig. 4. TEM images of SiO_2 NPs (a) and core-brush hybrid materials, (SiO_2-Cl)-*g*-PDEGMA, (b–c) (SiO_2-Br)-*g*-PDEGMA, (d–e) and (SiO_2-V)-*g*-PDEGMA, (f–g).

these particles scattered light strongly. Moreover, for SiO_2-Br, the particles aggregates are visible to the naked eye and settle down to bottom in a couple of hours, confirming an unstable colloid suspension.

Finally, the morphology of unmodified SiO_2 NPs and core-brush SiO_2 NPs with PDEGMA brushes was observed by TEM (Fig. 4). As the previous characterizations suggested, the unmodified SiO_2 NPs were found to be well dispersed spheres without aggregates.

TEM images from the final hybrid nanomaterial also showed marked differences depending on the kind of polymerization and initiator. For the (SiO_2-Cl)-*g*-PDEGMA NPs, Fig. 4(b–c), in agreement with results reported by DLS, we observed the coexistence of individual particles with polydisperse aggregates; although the surface grafting of PDEGMA was confirmed in previous experiments, the core-brush structure was not clearly observed by this technique. These hybrid NPs exhibited a difference in average external diameter of about 10 nm in comparison with bare SiO_2. The (SiO_2-Br)-*g*-PDEGMA, Fig. 4(d–e), presented a significant agglomeration with larger aggregates and, in good correlation with FTIR and TGA, clearly an organic layer could be observed due to the presence of the polymer. As no individual particles were found we could not inform any changes in the external diameter. However, the (SiO_2-V)-*g*-PDEGMA system resulted in well dispersed particles without distinguishable aggregation (see Fig. 4(f–g)). For these particles, it is clearly possible to appreciate the organic polymer layer of the core-brush structures. Typically, these NPs showed a difference in the average external diameter of approximately 16 nm in comparison to the naked SiO_2 NPs. In summary, TEM images confirm the results obtained from the previous techniques.

Scheme 2 depicts a representation of the aggregation degree and the superficial polymer content NPs during each synthesis step of the three different routes for core-brush nanomaterials. We hypothesize that the remarkable differences characteristics, in terms of aggregation and surface content, are a consequence of the involved synthesis process.

When the SI-ATRP pathways 1 and 2 are employed, uniform PDEGMA brushes were grafted on the SiO_2 surface. However, given that the starting colloids are aggregated (SiO_2-Cl and SiO_2-Br), one can expect that the morphology of the colloidal aggregates and their polymer content depends also on the surface reactivity. In Route 1, the less reactive CPTES-modified silica leads to lower grafting density, and as a consequence, relatively thin polymer shells are formed on the silica surfaces. In Route 2, however, the much higher reactivity triggered by BPATES leads to higher grafting density, and the thick synthesized polymer layer can eventually “engulf” these particle clusters. This suggests that the denser polymeric layer obtained using the more reactive BPATES initiator of SI-ATRP possibly contributes to the formation of macroscopic agglomerates. The limitations during the modification process make it very difficult to obtain the core-brush material resulting from this polymerization route as highly dispersed individual nanoparticles.

On the other hand, the approach of (SiO_2-V)-*g*-PDEGMA NPs preparation was carried out completely in ethanol solution. In this solvent, both unmodified and modified SiO_2 particles lead to stabilized sols. However, the percentage of synthesized polymeric layers is low in comparison with the core-brush obtained by SI-ATRP in pathway 2. It is important to notice that these results are in good agreement with a previous report by Kim and co-workers, [18] where they presented an improved and more effective preparation method for monodisperse poly methyl methacrylate–silica composites without agglomeration using UV-induced radical graft polymerization. Moreover, it was observed that the polymer content obtained by this route was similar to that of an SI-ATRP that employs the commercial and commonly used CPTES organic silane agent as the initiator.

It is important to notice that some methods, as SI-ATRP, require a complicated operation process, high demand of equipment, limitation of specific sensitive chemicals or high energy consumption, and an extra purification step (for example, the Cu catalyst complex removal), which corresponding economic costs do not have advantage or realistic feasibility for large-scale industrial production. In contrast, the UV-induced grafting polymerization exerts a relatively efficient, reproducible and simple process for PDEGMA brushes immobilization on the surface of SiO_2 NPs. These characteristics make it an attractive alternative to be extended to other materials and surfaces, and feasible to be scaled-up to higher production. [18,24]

As mentioned in the introduction, these hybrid core-brush materials can be tailor-made potentially with an unlimited number of architectures and in diverse forms, depending on the final requirements or its application. In this context, when obtaining core-brush NPs, it is essential to controlling the functionality incorporation and resulting morphological characteristics through the synthesis and processing

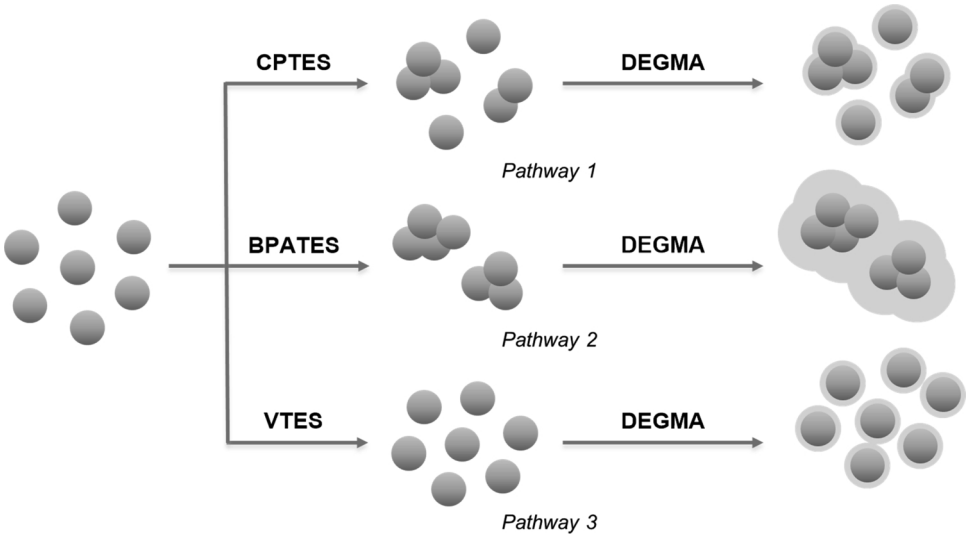

Scheme 2. Representation of the NPs aggregation during each step of synthesis.

techniques employed. In this framework, this report represents an important contribution in controlling the dispersion, polymer content and colloidal stability of silica-based hybrid nanoparticles. It was demonstrated that the selection of a synthesis methodology has a significant impact on these characteristics. Therefore, it is necessary, in the first place, to carry out a careful evaluation of the requirements of the nanomaterial depending on its final application before opting for one or another.

It is important to note that, these core-brush particles present high interest in different applications. First, the core-brush NPs were promising to be used as a thermo-responsive smart carrier. The results obtained here suggest that the LCST could be tuned choosing between one of our three pathway, because they conduced to different PDEGMA content on SiO_2 particles. The (SiO_2-Br)-*g*-PDEGMA is an especially interesting candidate due to the presence of a thicker tunable polymer shell and a clearly observable phase transition. Fig. 5 shows the behavior when (SiO_2-Br)-*g*-PDEGMA NPs colloid suspension was exposed to the temperature under stirring; a clear phase separation was immediately observed above the polymer LCST (close to 50 °C in this case), which was reversible when exposing to lower temperature values. Notice that, during this experiment the colloid suspension was under stirring, it means the particles were suspended.

On the other hand, due to the excellent hydration capability of the shells consisting of PEG brushes, the functional SiO_2 NPs can achieve good lubricating properties in aqueous media through hydration lubrication mechanism. [46] It is well known that it the surface modification with PEG groups helps to decrease the hemolytic activity of silica particles. PEG brushes not only mask the surface silanol groups but also serve as a protecting layer, hindering the contact of silica oligomers emerging from partially dissolved silica surfaces to the red blood cells RBCs. [47] Both systems (SiO_2-Cl)-*g*-PDEGMA and (SiO_2-V)-*g*-PDEGMA NPs, prepared by pathway 1 and 3 have a promising potential in this field. In addition, the vinyl pathway takes place entirely in ethanol solution, which leads to a simpler and efficient dispersion of the final product. It is worthy to note that the dilution of the initial ethanolic colloid in water leads to an excellent and stable dispersion.

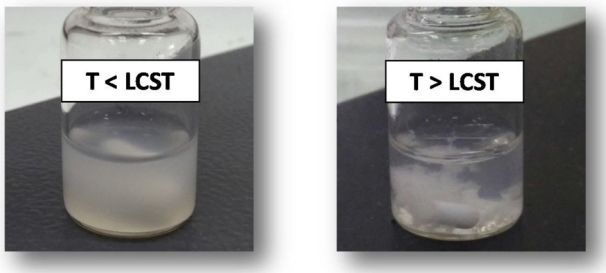

Fig. 5. Thermo-responsive behavior of (SiO_2-Br)-*g*-PDEGMA NPs.

In summary, we report for the first time a detailed study for the development and synthesis of core-brush nanoparticles via *grafting-from* approach on SiO_2 surface with PDEGMA-derived polymer brushes, using two types of radical polymerization, non-controlled and controlled. The results have demonstrated that the dispersion, stability, polymer content and object morphology of these PDEGMA-modified core-brush silica colloids can be controlled by tuning the experimental variables. In addition, the critical role of the preparation route has been highlighted. These hybrid colloids also present a temperature-responsive behavior, which makes them very promising for different applications in smart carriers.

4. Conclusions

Core-brush nanoparticles were designed and synthetized by *grafting-from* polymerization on SiO_2 surface with PDEGMA brushes. A crossed study by DRIFTS, TGA, TEM and DLS confirm the incorporation and nature of the polymers, and the possibility of controlling brush thickness, which in turn controls the aggregation process. We report three pathways for PDEGMA grafting on SiO_2 particles, involving two types of polymerization, non-controlled and controlled, which are different in synthesis complexity, experimental configuration, nanoparticles post-synthesis purification and polymer density grafted. These different alternatives led to core-brush nanoparticles with remarkable differences between them in terms of aggregation, surface charge and re-dispersability of the colloid systems. We concluded and suggest that the synthesis method for core-brush nanoparticles preparation should be selected depending on the requirements for the final material or its application. For example, if it is necessary to obtain a system with high content of polymer grafted on SiO_2 NPs, regardless of the way in which they are distributed or associated, we suggest used pathway 2. In case of lower content of polymer grafted on SiO_2 NPs, we recommend route 1 or 3. On the other hand, when a highly monodisperse final system and/or a straightforward method are relevant requirements, pathway 3 is the best selection. In addition, taking into account that the critical step of the methods presented here is the silica functionalization, we believe that these routes can be extended to monomers with similar reactivity, leading to PEG-modified (POEGMA or PEGMA) or acrylamide

(PNIPAm) backbones.

Acknowledgments

This work was made possible thanks to funding from UNSAM, MinCyT (PICT-2014-3687 and 2015-3526), and a CONICET-DFG joint project (MU 1674#15-1). Authors are also grateful to Gonzalo Zbihlei (CNEA) for his TEM assistance and Juan José Munafó (Fundación Argentina de Nanotecnología) for his collaboration in the photography edition of Fig. 3. M.J.P and C.B.C also acknowledges receipt of doctoral and postdoctoral fellowships from CONICET.

Appendix A. Supplementary data

Supplementary material related to this article can be found, in the online version, at doi:https://doi.org/10.1016/j.colsurfa.2019.04.035.

References

[1] C.-S. Ha, Polymer based hybrid nanocomposites; a progress toward enhancing interfacial interaction and tailoring advanced applications, Chem. Rec. 18 (2018) 759–775, https://doi.org/10.1002/tcr.201700030.
[2] S. Kango, S. Kalia, A. Celli, J. Njuguna, Y. Habibi, R. Kumar, Surface modification of inorganic nanoparticles for development of organic-inorganic nanocomposites - a review, Prog. Polym. Sci. 38 (2013) 1232–1261, https://doi.org/10.1016/j.progpolymsci.2013.02.003.
[3] S. Bashir, J. Liu, Nanomaterials and their application, Adv. Nanomater. Their Appl. Renew. Energy (2015) 1–50.
[4] G. Chen, I. Roy, C. Yang, P.N. Prasad, Nanochemistry and nanomedicine for nanoparticle-based diagnostics and therapy, Chem. Rev. 116 (2016) 2826–2885, https://doi.org/10.1021/acs.chemrev.5b00148.
[5] N. Dasgupta, S. Ranjan, C. Ramalingam, Applications of nanotechnology in agriculture and water quality management, Environ. Chem. Lett. 15 (2017) 591–605, https://doi.org/10.1007/s10311-017-0648-9.
[6] C. Sanchez, G.J. de, A.A. Soler-Illia, F. Ribot, T. Lalot, C.R. Mayer, V. Cabuil, Designed hybrid organic – inorganic nanocomposites from functional nanobuilding blocks, Chem. Mater. 13 (2001) 3061–3083, https://doi.org/10.1021/cm011061e.
[7] K. Shiba, M. Ogawa, Precise synthesis of well-defined inorganic-organic hybrid particles, Chem. Rec. 18 (2018) 950–968, https://doi.org/10.1002/tcr.201700077.
[8] P. Brown, H.B. Eral, Chapter 12 - Smart and Stimuli-responsive Colloids, (2016), https://doi.org/10.1016/B978-0-12-801578-0.00012-6.
[9] G.J.A.A. Soler-Illia, O. Azzaroni, Multifunctional hybrids by combining ordered mesoporous materials and macromolecular building blocks, Chem. Soc. Rev. 40 (2011) 1107, https://doi.org/10.1039/c0cs00208a.
[10] V.G. Ngo, C. Bressy, C. Leroux, A. Margaillan, Synthesis of hybrid TiO2 nanoparticles with well-defined poly(methyl methacrylate) and poly(tert-butyldimethylsilyl methacrylate) via the RAFT process, Polymer (Guildf) 50 (2009) 3095–3102, https://doi.org/10.1016/j.polymer.2009.04.077.
[11] C.B. Contreras, G. Chagas, M.C. Strumia, D.E. Weibel, Permanent superhydrophobic polypropylene nanocomposite coatings by a simple one-step dipping process, Appl. Surf. Sci. 307 (2014) 234–240, https://doi.org/10.1016/j.apsusc.2014.04.019.
[12] C.B. Contreras, F.N. Figueroa, D.E. Weibel, M.C. Strumia, Superhydrophobic polypropylene surfaces prepared with TiO2 nanoparticles functionalized by dendritic polymers, J. Polym. Sci. Part A: Polym. Chem. 56 (2018) 2019–2029, https://doi.org/10.1002/pola.29086.
[13] J.M. Goddard, J.H. Hotchkiss, Polymer surface modification for the attachment of bioactive compounds, Prog. Polym. Sci. 32 (2007) 698–725, https://doi.org/10.1016/j.progpolymsci.2007.04.002.
[14] D.W. Lee, B.R. Yoo, Advanced silica/polymer composites: materials and applications, J. Ind. Eng. Chem. 38 (2016) 1–12, https://doi.org/10.1016/j.jiec.2016.04.016.
[15] V. Vergnat, T. Roland, G. Pourroy, P. Masson, Effect of covalent grafting on mechanical properties of TiO 2/polystyrene composites, Mater. Chem. Phys. 147 (2014) 261–267, https://doi.org/10.1016/j.matchemphys.2014.04.038.
[16] T. Yamamoto, Y. Takahashi, Design of polymer particles maintaining dispersion stability for the synthesis of hollow silica particles through sol-gel reaction on polymer surfaces, Colloids Surf. A Physicochem. Eng. Asp. 553 (2018) 66–70, https://doi.org/10.1016/J.COLSURFA.2018.05.036.
[17] N. Tsubokawa, T. Kimoto, K. Koyama, Polymerization of vinyl monomers in the presence of silica having surface functional groups, Colloid Polym. Sci. 271 (1993) 940–946, https://doi.org/10.1007/BF00654853.
[18] S. Kim, E. Kim, S. Kim, W. Kim, Surface modification of silica nanoparticles by UV-induced graft polymerization of methyl methacrylate, J. Colloid Interface Sci. 292 (2005) 93–98, https://doi.org/10.1016/j.jcis.2005.09.046.
[19] Y.L. Khung, D. Narducci, Surface modification strategies on mesoporous silica nanoparticles for anti-biofouling zwitterionic film grafting, Adv. Colloid Interface Sci. 226 (2015) 166–186, https://doi.org/10.1016/j.cis.2015.10.009.
[20] J.M. Rosenholm, C. Sahlgren, M. Linden, Towards multifunctional, targeted drug delivery systems using mesoporous silica nanoparticles - opportunities & challenges, Nanoscale. 2 (2010) 1870–1883, https://doi.org/10.1039/c0nr00156b.
[21] K. Hamada, M. Kohri, T. Taniguchi, K. Kishikawa, In-situ assembly of diblock copolymers onto submicron-sized particles for preparation of core-shell and ellipsoidal particles, Colloids Surf. A Physicochem. Eng. Asp. 512 (2017) 80–86, https://doi.org/10.1016/J.COLSURFA.2016.10.035.
[22] J. Škvarla, J. Škvarla, A swellable polyelectrolyte gel-like layer on the surface of hydrous metal oxides in simple electrolyte solutions: hematite vs. silica colloids, Colloids Surf. A Physicochem. Eng. Asp. 513 (2017) 463–467, https://doi.org/10.1016/J.COLSURFA.2016.11.018.
[23] C. Padeste, S. Neuhaus, Functional polymer structures, Polym. Micro- Nanografting, William Andrew Publishing, 2015, pp. 1–10, https://doi.org/10.1016/B978-0-323-35322-9.00001-2.
[24] Q. Zhou, W. Luo, X. Zhang, Ingenious route for ultraviolet-induced graft polymerization achieved on inorganic particle: fabricating magnetic poly(acrylic acid) densely grafted nanocomposites for Cu2+ removal, Appl. Surf. Sci. 413 (2017) 181–190, https://doi.org/10.1016/j.apsusc.2017.04.033.
[25] C.M. Hui, J. Pietrasik, M. Schmitt, C. Mahoney, J. Choi, M.R. Bockstaller, K. Matyjaszewski, Surface-initiated polymerization as an enabling tool for multifunctional (Nano-)engineered hybrid materials, Chem. Mater. 26 (2014) 745–762, https://doi.org/10.1021/cm4023634.
[26] G. Huang, Z. Xiong, H. Qin, J. Zhu, Z. Sun, Y. Zhang, X. Peng, J. Ou, H. Zou, Synthesis of zwitterionic polymer brushes hybrid silica nanoparticles via controlled polymerization for highly efficient enrichment of glycopeptides, Anal. Chim. Acta 809 (2014) 61–68, https://doi.org/10.1016/j.aca.2013.11.049.
[27] V. Nguyen, W. Yoshida, J.D. Jou, Y. Cohen, Kinetics of free-radical graft polymerization of 1-vinyl-2-pyrrolidone onto silica, J. Polym. Sci. Part A: Polym. Chem. 40 (2002) 26–42, https://doi.org/10.1002/pola.10081.
[28] S. Khoonsap, T. Narkkun, P. Ratphonsan, S. Klinsrisuk, S. Amnuaypanich, Enhancing the grafting of poly(2-hydroxyethyl methacrylate) on silica nanoparticles (SiO2-g-PHEMA) by the sequential UV-induced graft polymerization with a multiple-UV irradiation, Adv. Powder Technol. 25 (2014) 1304–1310, https://doi.org/10.1016/j.apt.2014.03.010.
[29] Z. Du, X. Sun, X. Tai, G. Wang, X. Liu, Synthesis of hybrid silica nanoparticles grafted with thermoresponsive poly(ethylene glycol) methyl ether methacrylate via AGET-ATRP, RSC Adv. 5 (2015) 17194–17201, https://doi.org/10.1039/C4RA17013J.
[30] F.J. Xu, K.G. Neoh, E.T. Kang, Progress in Polymer Science Bioactive surfaces and biomaterials via atom transfer radical polymerization, Prog. Polym. Sci. 34 (2009) 719–761, https://doi.org/10.1016/j.progpolymsci.2009.04.005.
[31] A.Z. Wang, R. Langer, O.C. Farokhzad, Nanoparticle delivery of cancer drugs, Annu. Rev. Med. 63 (2012) 185–198, https://doi.org/10.1146/annurev-med-040210-162544.
[32] P. Mishra, B. Nayak, R.K. Dey, PEGylation in anti-cancer therapy: an overview, Asian J. Pharm. Sci. 11 (2016) 337–348, https://doi.org/10.1016/J.AJPS.2015.08.011.
[33] N. Hadjesfandiari, Stealth coatings for nanoparticles: polyethylene glycol alternatives, Eng. Biomater. Drug Deliv. Syst. (2018) 345–361, https://doi.org/10.1016/B978-0-08-101750-0.00013-1.
[34] Z. Du, X. Sun, X. Tai, G. Wang, X. Liu, Optimizing conditions of preparation of thermoresponsive SiO2-POEGMA particles via AGET-ATRP, Appl. Surf. Sci. 329 (2015) 234–239, https://doi.org/10.1016/j.apsusc.2014.12.107.
[35] Y. Shin, D. Lee, K. Lee, K.H. Ahn, B. Kim, Surface properties of silica nanoparticles modified with polymers for polymer nanocomposite applications, J. Ind. Eng. Chem. 14 (2008) 515–519, https://doi.org/10.1016/j.jiec.2008.02.002.
[36] S. Tugulu, A. Arnold, I. Sielaff, K. Johnsson, H.A. Klok, Protein-functionalized polymer brushes, Biomacromolecules 6 (2005) 1602–1607, https://doi.org/10.1021/bm050016n.
[37] W. Stöber, A. Fink, E. Bohn, Controlled growth of monodisperse silica spheres in the micron size range, J. Colloid Interface Sci. 26 (1968) 62–69, https://doi.org/10.1016/0021-9797(68)90272-5.
[38] V.M. Masalov, N.S. Sukhinina, E.A. Kudrenko, G.A. Emelchenko, Mechanism of formation and nanostructure of Stober silica particles, Nanotechnology 22 (2011) 275718, https://doi.org/10.1088/0957-4484/22/27/275718.
[39] A. van Blaaderen, A.P.M. Kentgens, Particle morphology and chemical microstructure of colloidal silica spheres made from alkoxysilanes, J. Non. Solids 149 (1992) 161–178, https://doi.org/10.1016/0022-3093(92)90064-Q.
[40] K. Matyjaszewski, Atom transfer radical polymerization (ATRP): current status and future perspectives, Macromolecules 45 (2012) 4015–4039.
[41] L.T. Zhuravlev, The surface chemistry of amorphous silica. Zhuravlev model, Colloids Surf. A Physicochem. Eng. Asp. 173 (2000) 1–38.
[42] A.Y. Fadeev, T.J. McCarthy, Self-Assembly Is Not the Only Reaction Possible Between Alkyltrichlorosilanes and Surfaces: Monomolecular and Oligomeric Covalently Attached Layers of Dichloro- and Trichloroalkylsilanes on Silicon, (2000), https://doi.org/10.1021/la000471z.
[43] A. Van Blaaderen, A. Vrij, Synthesis and characterization of colloidal dispersions of fluorescent, monodisperse silica spheres, Langmuir 8 (1992) 2921–2931, https://doi.org/10.1021/la00048a013.
[44] M. Pálmai, L.N. Nagy, J. Mihály, Z. Varga, G. Tárkányi, R. Mizsei, I.C. Szigyártó, T. Kiss, T. Kremmer, A. Bóta, Preparation, purification, and characterization of aminopropyl-functionalized silica sol, J. Colloid Interface Sci. 390 (2013) 34–40, https://doi.org/10.1016/J.JCIS.2012.09.025.
[45] M.J. Penelas, G.J.A.A. Soler-Illia, V. Levi, A.V. Bordoni, A. Wolosiuk, Click-based thiol-ene photografting of COOH groups to SiO2 nanoparticles: strategies comparison, Colloids Surf. A Physicochem. Eng. Asp. 562 (2019) 61–70, https://doi.org/10.1016/J.COLSURFA.2018.11.023.
[46] G. Liu, M. Cai, F. Zhou, W. Liu, Charged polymer brushes-grafted hollow silica nanoparticles as a novel promising material for simultaneous joint lubrication and treatment, J. Phys. Chem. B 118 (2014) 4920–4931, https://doi.org/10.1021/jp500074g.
[47] Y.-S. Lin, C.L. Haynes, Impacts of mesoporous silica nanoparticle size, pore ordering,and pore integrity on hemolytic activity, J. Am. Chem. Soc. 132 (2010) 4834–4842, https://doi.org/10.1021/ja910846q.